

# Steam reforming of methanol on copper catalysts supported on large-surface-area $ZnAl_2O_3$

Tatsuya Takeguchi <sup>\*</sup>, Yukimune Kani, Masashi Inoue, and Koichi Eguchi

Department of Energy and Hydrocarbon Chemistry, Graduate School of Engineering, Kyoto University, Sakyo-ku, Kyoto 606-8501, Japan

Received 12 January 2002; accepted 29 May 2002

Steam reforming of methanol on various supported Cu catalysts was examined. Supports strongly affected catalyst activity and, among the catalysts tested, Cu catalyst supported on large-surface-area  $ZnAl_2O_4$  showed the highest activity, which, to the best of our knowledge, was higher than those for the supported catalysts reported so far. For supported Cu catalysts, two species were observed. One was a dispersed Cu species having strong interaction between Cu and support, and the other was an isolated Cu species. The activity of the former species strongly depended on supports.

**KEY WORDS:** supported Cu catalyst; large-surface-area  $ZnAl_2O_3$ ; steam reforming of methanol; hydrogen production.

## 1. Introduction

Recently, much attention has been paid to steam reforming of methanol ( $CH_3OH + H_2O \rightarrow 3H_2 + CO_2$ ) to produce the hydrogen for fuel cells. Many catalysts have been reported in the literature [1–5], and the majority of them are copper-containing catalysts prepared by the co-precipitation method [1–5]. Supported Cu catalysts prepared by the impregnation method [6,7], the kneading method [8–10] and ion exchange [9,11] have also been reported; however, their activities were not high because of the difficulty in dispersing Cu particles stably.

It is generally accepted that turnover frequency (TOF) and selectivity are affected by copper-particle sizes and increase with an increase in copper-particle radius up to 5 nm [9]. The large copper particles show high TOF and high selectivity to  $CO_2$ , but TOF does not depend on supports or copper-particle radius [12].

In this report, supported Cu catalysts were prepared by impregnation methods. Catalysts were characterized by XRD, TPR and FTIR, and the nature of Cu active sites will also be discussed.

## 2. Experimental

### 2.1. Catalyst preparation

Various kinds of supports,  $ZnAl_2O_4$ ,  $ZnGa_2O_4$  and  $ZnO$ , were prepared by the glycothermal method [13] and calcined at 400 °C for 30 min in air, which is denoted

GT. For the reference,  $Al_2O_3$  (JRC-ALO-4) was used, which was calcined at 1060 °C for 30 min in air prior to use. For comparison,  $ZnAl_2O_4$  was also prepared by co-precipitation from a mixed metal nitrate solution [14]. The pH of the solution (initial pH, 2) was brought to 7.5 by the addition of a 20 wt% aqueous solution of ammonium carbonate. The gelatinous precipitate was washed with water and then calcined at 800 °C for 6 h in air. The resulting powders were denoted as  $ZnAl_2O_4(Cp)$ .

Supported Cu catalysts were prepared by the wet impregnation technique using an aqueous solution of copper formate. After loading, the samples were dried at 80 °C and calcined at 350 °C for 30 min in air.

A co-precipitated Cu/Zn/Al mixed oxide catalyst was prepared as follows: to 100 ml of 1.2 M  $NaHCO_3$  solution (pH 8.2), 50 ml of a mixed  $Cu(NO_3)_2/Zn(NO_3)_2/Al(NO_3)_3$  solution (1.0 M as  $NO_3^-$ ) was added dropwise over 20 min at 65 °C with stirring. The formed precipitates were aged at the same temperature for 90 min under continuous stirring, then filtered, washed with water, dried at 120 °C overnight, and calcined at 350 °C in air for 30 min. The thus-obtained catalyst is designated Cu–Zn–Al(Cp).

### 2.2. Characterization of the catalysts

The XRD measurement was carried out on a Shimadzu XD-D1 diffractometer using  $Cu K_\alpha$  radiation and a carbon monochromator. The TPR run was carried out using 25 mg of the catalyst from room temperature to 400 °C at a heating rate of 10 °C/min in a 25 ml/min flow of 5%  $H_2$ –95% Ar. To measure the surface area of Cu particles,  $N_2O$  titration ( $N_2O + 2Cu_s \rightarrow Cu_s - O - Cu_s + N_2$ ) was carried out at 100 °C by the ordinary pulse method.

<sup>\*</sup> To whom correspondence should be addressed.  
E-mail: takeguchi@scl.kyoto-u.ac.jp

The BET surface area was measured on a Micromeritics FlowSorb II 2300 by N<sub>2</sub> uptake at the liquid nitrogen temperature.

The FTIR spectra were recorded on a Nicolet MAGNA-IR 560 spectrometer. The catalysts were heated to 250 °C at rate of 24 °C/min in a 20 ml/min flow of 50% He–50% H<sub>2</sub> and kept for 10 min. After cooling down to 25 °C, the catalysts were flushed with a 30 ml/min He flow at 25 °C for 5 min. Then, FTIR spectra of adsorbed CO were recorded in a 40 ml/min flow of 2.5% CO–97.5% He.

### 2.3. Reaction method

Steam reforming of methanol was carried out at atmospheric pressure using a conventional flow system. The catalyst was tableted and pulverized to 20–14 mesh, and 100 mg of catalyst was set in the reactor. Prior to the reaction, each catalyst was *in situ* pretreated in an 8.7% H<sub>2</sub>/N<sub>2</sub> stream at 250 °C for 30 min. A gas mixture composed of 52% N<sub>2</sub>, 24% CH<sub>3</sub>OH and 24% H<sub>2</sub>O was allowed to flow at the rate of 250 ml(STP)/min (*W/F* = 0.024 g s/ml). Reaction products were analyzed using an on-line gas chromatograph (Chromopack, Micro-GC CP2002).

## 3. Results and discussion

### 3.1. XRD

Figure 1 shows the comparison of Cu/(Zn + Al) atomic ratios charged and calculated by XRD on the basis of peak intensity ratio of standard mixtures of Cu and support. Every plot for the support has a small *x*-intercept, suggesting that two-type Cu species were present in the catalysts. One is an isolated Cu species detectable by XRD, and the other is a dispersed Cu

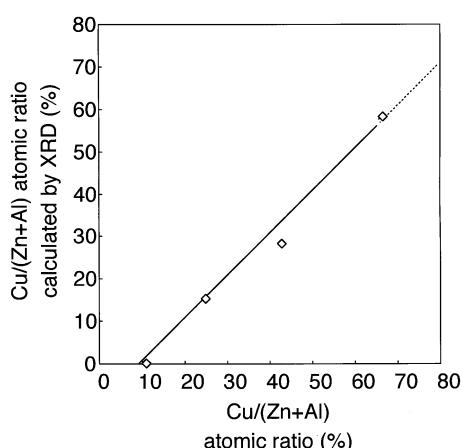


Figure 1. Comparison of Cu/(Zn + Al) atomic ratios charged and calculated by XRD.

species that cannot be detected by XRD. The amount of Cu species dispersed on ZnAl<sub>2</sub>O<sub>4</sub> was estimated from the intercept in figure 1, and results are shown in table 1. Similarly the amounts of the Cu species dispersed on the other supports were also obtained, and results are also shown in table 1. Although 10 mol% Cu catalysts predominantly consisted of dispersed Cu species, both species were present for the catalyst containing over 20 mol% Cu.

Table 1 lists the crystallite size and particle diameter of metallic Cu of the catalysts. The amount of exposed Cu for the dispersed Cu species was estimated from 20 mol% Cu samples (10 mol% Cu for ZnO) assuming that Cu components consisted of dispersed Cu species and single-crystal isolated Cu species. With an increase in the Cu loading, both the crystallite and particle sizes of isolated Cu species increased. However, for the 30 and 40 mol% Cu catalysts, the particle size of isolated Cu species was larger than the crystallite size. This indicates that most of the isolated Cu species were divided into smaller crystallites, although a small amount of Cu was dispersed on the support.

### 3.2. Temperature-programmed reactions

Figure 2 shows the TPR profiles of CuO/ZnAl<sub>2</sub>O<sub>4</sub> catalysts. For the 10 mol% CuO catalyst, most of the CuO was reduced at under 260 °C, indicating that CuO species dispersed on ZnAl<sub>2</sub>O<sub>4</sub> were easily reduced. For the high Cu-loading catalysts, the peak temperature for reduction of isolated CuO particles shifts toward higher temperature. A shoulder peak was clearly observed at around 230 °C where the 10 mol% Cu catalyst exhibited the peak, and the amounts of dispersed Cu species were essentially identical irrespective of Cu loadings. This also indicated that a certain amount of dispersed Cu species is present in high Cu-loading samples.

### 3.3. Infrared spectra of CO chemisorbed on the supported Cu catalysts

Figure 3 shows the IR spectra of CO adsorbed onto the Cu catalysts. For 10 mol% Cu/ZnAl<sub>2</sub>O<sub>4</sub>, a band was observed at 2107 cm<sup>-1</sup>. For a high Cu-loading catalyst on ZnAl<sub>2</sub>O<sub>4</sub>, two bands were observed at 2170 cm<sup>-1</sup> and 2107 cm<sup>-1</sup>, and the proportion of the band at 2170 cm<sup>-1</sup> increased with an increase in Cu loading. These data indicated that the band at 2107 cm<sup>-1</sup> was attributed to the dispersed Cu species, while the band at 2170 cm<sup>-1</sup> was attributed to the isolated Cu species. It was suggested that the band at 2170 cm<sup>-1</sup> was related to CO adsorbed onto surface Cu<sup>+</sup> species [15]. Since our TPR results indicate that the isolated CuO species was not easily reduced, some part of Cu remained as Cu<sup>+</sup> after in-site reduction, which gave the 2170 cm<sup>-1</sup> band.

Table 1  
Characteristics of dispersed Cu species and isolated Cu species.

Catalyst (mol% Cu)	Dispersed Cu species		Isolated Cu species			
	Cu amount <sup>a</sup> (mmol/g-support)	Exposed Cu <sup>b</sup> (mmol/g-support)	Cu amount (mmol/g-support)	Exposed Cu (mmol/g-support)	Crystallite size <sup>c</sup> (nm)	Particle size <sup>d</sup> (nm)
<b>ZnAl<sub>2</sub>O<sub>4</sub>(GT)</b>						
10	1.45	0.07	0.36	0.11	—	—
20	1.45	0.07	2.64	0.22	15	15
30	1.45	0.07	5.56	0.10	21	75
40	1.45	0.07	9.45	0.11	26	106
<b>ZnGa<sub>2</sub>O<sub>4</sub></b>						
10	1.24	0.14	—	—	—	—
20	1.67	0.08	1.12	0.05	26	26
30	1.67	0.08	3.11	0.07	26	56
40	1.67	0.08	5.77	0.13	35	57
<b>ZnO</b>						
10	0.55	0.13	0.82	0.02	42	42
20	0.55	0.13	2.53	0.06	35	50
30	0.55	0.13	4.72	0.08	32	77
40	0.55	0.13	7.65	0.02	47	440
<b>Al<sub>2</sub>O<sub>3</sub></b>						
10	1.74	0.08	0.44	0.03	—	18
20	1.74	0.08	3.16	0.13	30	30
30	1.74	0.08	6.66	0.03	33	270
40	1.74	0.08	11.3	0.04	38	380

<sup>a</sup> The amount of dispersed Cu species was estimated by the XRD plots similar to figure 1.

<sup>b</sup> The amount of exposed Cu for dispersed Cu species was estimated from 20 mol% Cu samples (10 mol% Cu for ZnO) assuming that Cu components consisted of dispersed Cu and single-crystal isolated Cu species.

<sup>c</sup> The crystallite size was obtained for the 111 peak by the Sherrer equation.

<sup>d</sup> The particle size was calculated by the result of N<sub>2</sub>O titration, assuming that one Cu atom of the particles occupies a surface area of 0.0568 nm<sup>2</sup> (= 2 $\sqrt{3}r_{\text{cu}}^2$ , where  $r_{\text{cu}}$  is the atomic radius of Cu). When the total surface area of Cu particles was expressed as  $S$  (0.0568 nm<sup>2</sup>  $\times$  number of surface Cu), the diameter of Cu particles,  $D$ , was calculated to be  $6V/S$  ( $V$  is the total volume of Cu).

### 3.4. Steam reforming of methanol

Characteristics and performances of Cu catalysts are compared in table 2. The isolated Cu species with low dis-

persion tended to show higher TOF than that with high dispersion. The catalytic activity of Cu/ZnAl<sub>2</sub>O<sub>4</sub>(GT) was higher than that of Cu/ZnAl<sub>2</sub>O<sub>4</sub>(Cp), indicating that the large surface area of ZnAl<sub>2</sub>O<sub>4</sub>(GT) is effective

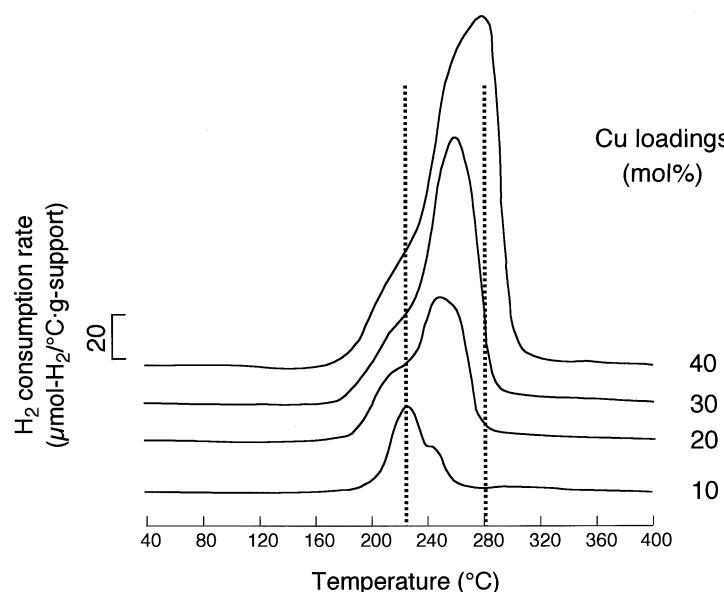


Figure 2. TPR profile of CuO/ZnAl<sub>2</sub>O<sub>4</sub> with various Cu loadings. Sample, 25 mg; feed gas, 5% H<sub>2</sub>–95% Ar; flow rate, 25 ml/min; heating rate, 10 °C/min.

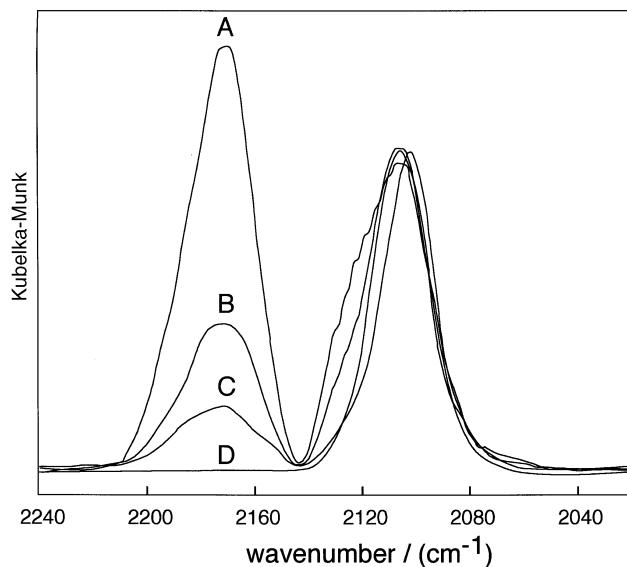


Figure 3. FTIR spectra of CO adsorbed on CuO/ZnAl<sub>2</sub>O<sub>4</sub> with various Cu loadings. Feed gas, 2.5% CO–97.5% Ar; flow rate; 40 ml/min, temperature, 25 °C. (A) 40 mol% Cu, (B) 30 mol% Cu, (C) 20 mol% Cu, (D) 10 mol% Cu.

for improvement of the catalytic performance. In this paper, 30 mol% Cu/ZnAl<sub>2</sub>O<sub>4</sub>(GT) shows the highest conversion among the catalysts tested, and its performance was compared with those of the catalysts reported in the literature [1,4–6,10,11,16,17] (figure 4). As shown in figure 4, this present catalyst showed a much higher H<sub>2</sub> production rate than the supported Cu catalysts examined so far and exhibited an equivalent activity to the co-precipitation catalyst.

The activation energy was determined from the Arrhenius plot of methanol conversions on 10 and 30 mol% Cu catalysts supported on ZnAl<sub>2</sub>O<sub>4</sub>(GT), ZnGa<sub>2</sub>O<sub>4</sub>, ZnO and Al<sub>2</sub>O<sub>3</sub>(cal.), and results are shown in table 3. Since the contribution of dispersed Cu species was dominant for the methanol conversion for 10 mol% Cu catalysts, the activation energy strongly depended on supports, indicating that there is strong interaction between Cu and supports. The Cu/ZnAl<sub>2</sub>O<sub>4</sub>(GT) showed the highest conversion (9.7%) and the lowest activation energy (89.7 kJ/mol), while the Cu/ZnO showed the lowest conversion and the highest activation energy.

Table 2  
Characteristics and performance for steam reforming catalysts of methanol.<sup>a</sup>

Catalyst (mol% Cu)	BET surface area (m <sup>2</sup> /g)	MeOH conversion (%)	Specific rate (mmol-MeOH converted/h g-support)	TOF (s <sup>-1</sup> )		Dispersion of isolated Cu species (%)
				Dispersed Cu species	Isolated Cu species	
<b>ZnAl<sub>2</sub>O<sub>4</sub>(GT)</b>						
10	215	9.7	178	0.68	–	30.9
20	225	11.4	243	0.68	0.08	8.4
30	152	13.2	330	0.68	0.44	1.7
40	126	12.5	375	0.68	0.48	1.1
<b>ZnAl<sub>2</sub>O<sub>4</sub>(Cp)</b>						
30	24	4.5	113	1.02 <sup>c</sup>	–	0.4 <sup>c</sup>
<b>Cu/Zn/Al (Cp)<sup>b</sup></b>						
45	100	11.4	340	0.10 <sup>c</sup>	–	8.9 <sup>c</sup>
<b>ZnGa<sub>2</sub>O<sub>4</sub></b>						
10	70	6.7	118	0.24	–	–
20	66	7.9	155	0.41	0.20	4.9
30	57	5.8	129	0.41	0.04	2.2
40	51	5.5	141	0.41	0.05	2.2
<b>ZnO</b>						
10	6	0.3	5	0.01	–	3.0
20	8	1.9	38	0.01	0.14	2.5
30	10	2.8	64	0.01	0.21	1.6
40	7	2.6	69	0.01	0.82	0.3
<b>Al<sub>2</sub>O<sub>3</sub> (cal.)</b>						
10	114	7.2	136	0.48	–	7.1
20	109	8.1	181	0.48	0.09	4.2
30	79	6.3	169	0.48	0.29	0.5
40	66	5.8	190	0.48	0.38	0.3
<b>Al<sub>2</sub>O<sub>3</sub></b>						
30	97	5.7	158	0.22 <sup>c</sup>	–	2.4 <sup>c</sup>

<sup>a</sup> Reaction conditions: catalyst: 100 mg; N<sub>2</sub> 130 ml/min, CH<sub>3</sub>OH 60 ml/min, H<sub>2</sub>O 60 ml/min; W/F = 0.024 g s/ml, 230 °C.

<sup>b</sup> Cu/Zn/Al (mol%), 45:45:10.

<sup>c</sup> Averaged values of both Cu species.

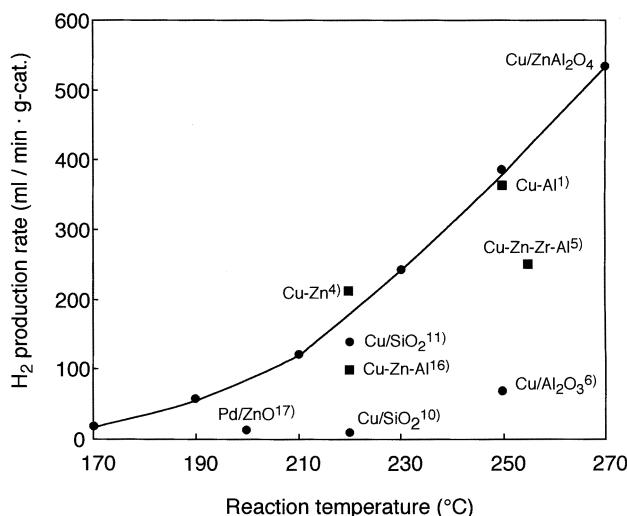


Figure 4. Comparison of catalytic performances for steam reforming of methanol. (●) Impregnation catalyst; (■) co-precipitation catalyst.

On the other hand, for 30 mol% Cu catalysts, the isolated Cu species affected the methanol conversion, and the activation energies are essentially identical to *ca.* 89 kJ/mol, irrespective of supports, although the ZnAl<sub>2</sub>O<sub>4</sub>(GT)-supported catalyst still exhibited the lowest activation energy and the highest number of exposed Cu of isolated species. On the contrary, for the ZnO support, the activation energy depended on the Cu loadings, since Cu/ZnO had the lowest number of exposed Cu of isolated species. These results indicate that the supports affected the particle sizes of isolated

Table 3  
Activation energy of methanol steam reforming on Cu catalysts supported on various supports.

Cu loading (mol %)	Activation energy (kJ/mol)			
	ZnAl <sub>2</sub> O <sub>4</sub> (GT)	ZnGa <sub>2</sub> O <sub>4</sub>	ZnO	Al <sub>2</sub> O <sub>3</sub> (cal.)
10	89.7	93.2	119	98.8
30	87.8	91.7	89.3	89.7

Cu species, but hardly affected the nature of the isolated Cu species. The ZnAl<sub>2</sub>O<sub>4</sub>(GT) support with high surface area was the most suitable among the supports tested in this paper.

#### 4. Conclusions

For high Cu-loading catalysts, two Cu species were observed. One was a Cu species dispersed on the support, and the other was an isolated Cu species. The activity of dispersed Cu species strongly depended on supports. Both of the Cu species contributed to the methanol conversion. The 30 mol% Cu/ZnAl<sub>2</sub>O<sub>4</sub>(GT) shows the highest H<sub>2</sub> production rate for supported Cu catalysts in the literature, which was rather higher than the co-precipitation catalyst.

#### References

- [1] M. Matsukata, S. Uemura and E. Kikuchi, Chem. Lett. (1988) 761.
- [2] R.O. Idem and N.N. Bakhshi, Ind. Eng. Chem. Res. 33 (1944) 2047.
- [3] R.O. Idem and N.N. Bakhshi, Ind. Eng. Chem. Res. 34 (1995) 1548.
- [4] G. Shen, S. Fujita, S. Matsumoto and N. Takezawa, J. Mol. Catal. A 124 (1997) 123.
- [5] J.P. Breen and J.R.H. Ross, Catal. Today 51 (1999) 521.
- [6] T. Inui, M. Suehiro and Y. Takegami, J. Jpn. Petrol. Inst. 25 (1982) 63.
- [7] H. Agaras and G. Cerrella, Appl. Catal. 45 (1988) 53.
- [8] C. Minochi, H. Kobayashi and N. Takezawa, Chem. Lett. (1979) 507.
- [9] H. Kobayashi, N. Takezawa, C. Minochi and K. Takahashi, Chem. Lett. (1980) 1197.
- [10] H. Kobayashi, N. Takezawa and C. Minochi, J. Catal. 69 (1981) 487.
- [11] N. Takezawa, H. Kobayashi, A. Hirose, M. Shimokawabe and K. Takahashi, Appl. Catal. 4 (1982) 127.
- [12] N. Takezawa, Shokubai 37 (1995) 320.
- [13] M. Inoue, H. Otsu, H. Kominami and T. Inui, Nippon Kagaku Kaishi (1991) 1036.
- [14] M.A. Valenzuela, J.-P. Jacobs, P. Bosch, S. Reijne, B. Zapata and H.H. Brongersma, Appl. Catal. A 148 (1997) 315.
- [15] M.A. Kohler, N.W. Cant, M.S. Wainwright and D.L. Trimm, J. Catal. 117 (1989) 188.
- [16] K. Miyao, H. Onodera and N. Takezawa, React. Kinet. Catal. Lett. 53 (1994) 379.
- [17] N. Iwasa, S. Kudo, H. Takahashi, S. Matsuda and N. Takezawa, Catal. Lett. 19 (1993) 211.